

## Factors Involved in the Formation of Amorphous and Crystalline Calcium Carbonate: A Study of an Ascidian Skeleton

Joanna Aizenberg,<sup>\*,†</sup> Gretchen Lambert,<sup>‡</sup> Steve Weiner,<sup>§</sup> and Lia Addadi<sup>§</sup>

Contribution from the Bell Laboratories/Lucent Technologies, 600 Mountain Avenue, Murray Hill, New Jersey 07974, Department of Biological Science, California State University, Fullerton, California 92634, and Department of Structural Biology, Weizmann Institute of Science, Rehovot 76100, Israel

Received August 31, 2001

**Abstract:** The majority of invertebrate skeletal tissues are composed of the most stable crystalline polymorphs of CaCO<sub>3</sub>, calcite, and/or aragonite. Here we describe a composite skeletal tissue from an ascidian in which amorphous and crystalline calcium carbonate coexist in well-defined domains separated by an organic sheath. Each biogenic mineral phase has a characteristic Mg content (5.9 and 1.7 mol %, respectively) and concentration of intramineral proteins (0.05 and 0.01 wt %, respectively). Macromolecular extracts from various biogenic amorphous calcium carbonate (ACC) skeletons are typically glycoproteins, rich in glutamic acid and hydroxyamino acids. The proteins from the crystalline calcitic phases are aspartate-rich. Macromolecules extracted from biogenic ACC induced the formation of stabilized ACC and/or inhibited crystallization of calcite in vitro. The yield of the synthetic ACC was 15–20%. The presence of Mg facilitated the stabilization of ACC: the protein content in synthetic ACC was 0.12 wt % in the absence of Mg and 0.07 wt % in the presence of Mg (the Mg content in the precipitate was 8.5 mol %). In contrast, the macromolecules extracted from the calcitic layer induced the formation of calcite crystals with modified morphology similar to that expressed by the original biogenic calcite. We suggest that specialized macromolecules and magnesium ions may cooperate in the stabilization of intrinsically unstable amorphous calcium carbonate and in the formation of complex ACC/calcite tissues in vivo.

### Introduction

The ability of organisms to exert an astonishing level of control over mineral deposition is illustrated by the biological formation and stabilization of amorphous calcium carbonate<sup>1,2</sup> (ACC)—a phase which is intrinsically unstable thermodynamically and kinetically at physiological pH, temperature, and pressure.<sup>3,4</sup>

When formed in vitro as a result of excessive supersaturation in the solution, ACC is rapidly transformed into the most stable crystalline polymorph of calcium carbonate, calcite.<sup>5</sup> Stabilization of metastable phases in vitro can be achieved by the direct inhibition of the formation of nuclei of crystallization of the

more stable phases by specialized additives.<sup>6</sup> It has been shown that hydroxy-containing molecules present in a crystallizing solution stabilize amorphous calcium carbonate at low temperatures.<sup>7</sup> Formation of ACC was also observed when poly(propylene imine) dendrimers modified with long alkyl chains were introduced into calcium carbonate solution.<sup>8</sup> The additives must be active at the nanoscopic level in the entire solution. Therefore, a relatively high concentration is required.<sup>9</sup>

The instability and therefore ease of redissolution of ACC is probably one reason for its formation in biology, judging from the fact that various organisms in different taxonomic groups use ACC as a temporary storage site for calcium and carbonate.<sup>1–3</sup> Surprisingly however, the formation of stabilized ACC for structural purposes is also observed in nature.<sup>10</sup> Examples are the cystoliths in leaves of certain plants,<sup>11,12</sup> exoskeletons of crustaceans,<sup>1,13</sup> and ascidians (a group within the *Chordata*).<sup>14,15</sup>

<sup>†</sup> Bell Laboratories/Lucent Technologies.

<sup>‡</sup> California State University.

<sup>§</sup> Weizmann Institute of Science.

- (1) Lowenstam, H. A.; Weiner, S. *On Biomineralization*; Oxford University Press: New York, 1989.
- (2) Watabe, N.; Meenakshi, V. R.; Blackwelder, P. L.; Kurtz, E. M.; Dunkelberger, D. G. In *Mechanisms of Biomineralization in the Invertebrates and Plants*; Watabe, N., Wilbur, K. M., Eds.; University of South Carolina Press: Columbia, SC, 1976; pp 283–308.
- (3) Nancollas, G. H. In *Biomineralization. Chemical and Biochemical Perspectives*; Mann, S., Webb, J., Williams, R. J. P., Eds.; VCH Publishers: Weinheim, 1989; pp 157–187.
- (4) (a) Clarkson, J. R.; Price, T. J.; Adams, C. J. *J. Chem. Soc., Faraday Trans. 1992*, **88**, 243–249. (b) Koga, N.; Nakagoe, Y.; Tanaka, H. *Thermochim. Acta* **1998**, **318**, 239–244.
- (5) (a) Brecevic, L.; Nielsen, A. *J. Cryst. Growth* **1989**, **98**, 504–510. (b) Kojima, Y.; Kawanobe, A.; Yasue, T.; Arai, Y. *J. Ceram. Soc. Jpn.* **1993**, **101**, 1145–1152.

- (6) (a) Becker, G. L.; Chen, C. H.; Greenwalt, J. W.; Lehninger, A. L. *J. Cell Biol.* **1974**, **61**, 316–321. (b) Posner, A. S.; Betts, F.; Blumenthal, N. C. *Metab. Bone Dis. Relat. Res.* **1978**, **1**, 179–184.
- (7) Merten, H. L.; Bachman, G. L. U.S. Patent 4,237,147, 1980.
- (8) Donners, J.; Heywood, B. R.; Meijer, E. W.; Nolte, R. J. M.; Roman, C.; Schenning, A.; Sommerdijk, N. *Chem. Commun.* **2000**, **19**, 1937–1938.
- (9) (a) Gower, L. B.; Odom, D. J. *J. Cryst. Growth* **2000**, **210**, 719–734. (b) Xu, G. F.; Yao, N.; Aksay, I. A.; Groves, J. T. *J. Am. Chem. Soc.* **1998**, **120**, 11977–11985.
- (10) Lowenstam, H. A. *Bull. Mar. Sci.* **1989**, **45**, 243–252.
- (11) Setoguchi, H.; Okazaki, M.; Suga, S. In *Origin, Evolution, and Modern Aspects of Biomineralization in Plants and Animals*; Crick, R. E., Ed.; Plenum Press: New York, 1989; pp 409–418.

A combination of stabilized ACC and calcite is used for the construction of skeletal spicules by the calcareous sponge *Clathrina*.<sup>15</sup> The sea urchin larval spicule also contains both ACC and a single crystal of calcite, but in this case the ACC is a transient precursor phase of the more stable calcite.<sup>16,17</sup>

Specialized macromolecules are found within calcium carbonate formed by many organisms.<sup>1,18,19</sup> It has been shown that they are the key components controlling various properties of biogenic minerals, such as shaping the sophisticated morphology of biogenic single calcite crystals during growth<sup>20</sup> and regulation of their mechanical<sup>21</sup> and textural<sup>22,23</sup> properties. We have also shown in vitro that specialized macromolecules are involved in the formation of stabilized ACC.<sup>15</sup> Another characteristic component of biogenic calcium carbonate phases is magnesium. In many cases, magnesium contents are higher than the maximum value compatible with thermodynamically stable magnesian calcite.<sup>1</sup> It has also been shown that Mg ions may be involved in the stabilization of unstable amorphous phases, such as ACC and amorphous calcium phosphate.<sup>6,24</sup> It is of interest to note that phosphate is often present in addition to Mg in ACC-bearing mineralized tissues.<sup>13</sup> It is not known whether macromolecules, phosphate, and magnesium cooperate in the formation and/or stabilization of amorphous and crystalline skeletal elements in vivo.

Here we present a detailed study of a skeletal element composed of both ACC and calcite. These are the tunic spicules (also called “dogbone” spicules due to their peculiar shape) formed by the ascidian *Pyura pachydermatina*. The body spicules (so-called “antler” spicules) produced by the same organism are composed entirely of ACC.<sup>14,15</sup> They contain a number of macromolecules, some of which are able to stabilize ACC in vitro.<sup>15</sup> Here we describe the structure and composition of the tunic spicules and compare them with the body spicules. We also investigate the effect that the macromolecules associated with these amorphous and crystalline phases have on the formation of calcite and stabilized ACC in vitro.

## Experimental Section

**Materials.** Solitary ascidians *Pyura pachydermatina* (Urochordata, Ascidiacea) were collected from shallow submerged rocks in Otago Harbor, New Zealand. Skeletal spicules were isolated on site: body (antler) spicules (Figure 1) were isolated from the branchial sac tissue in 5.25% sodium hypochlorite solution for 10–20 min to remove extraskeletal organic tissue; to obtain the tunic (dogbone) spicules

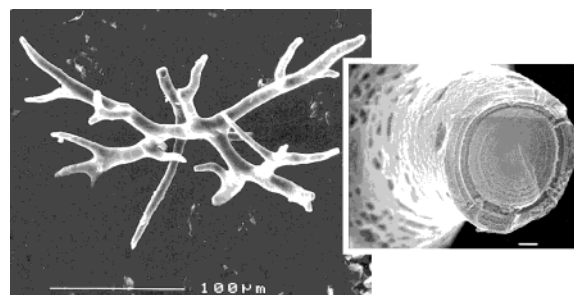


**Figure 1.** Body (antler) spicule formed by the ascidian *Pyura pachydermatina*. Inset: Etch figures after KOH treatment.

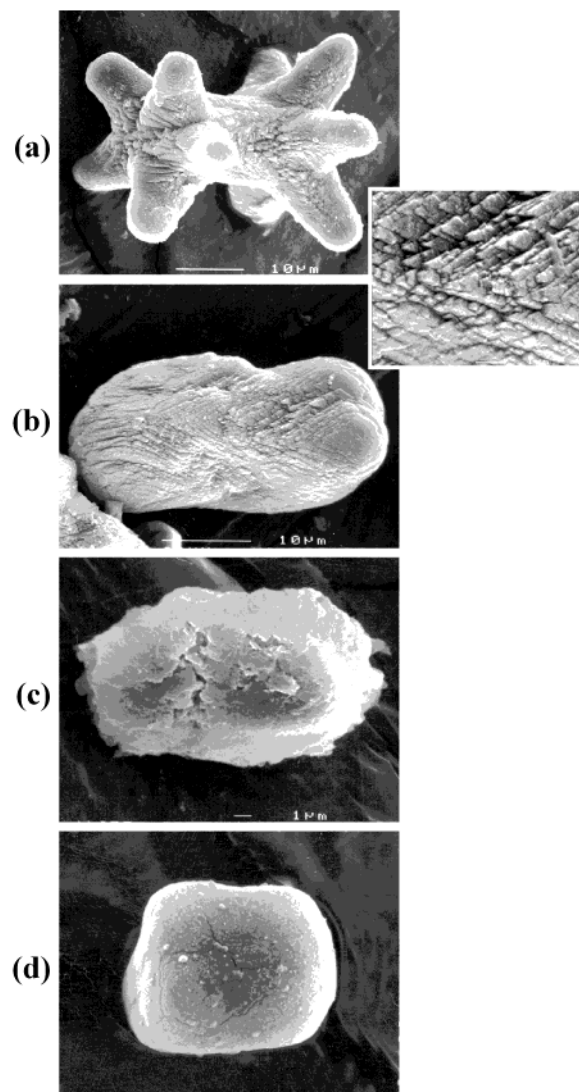


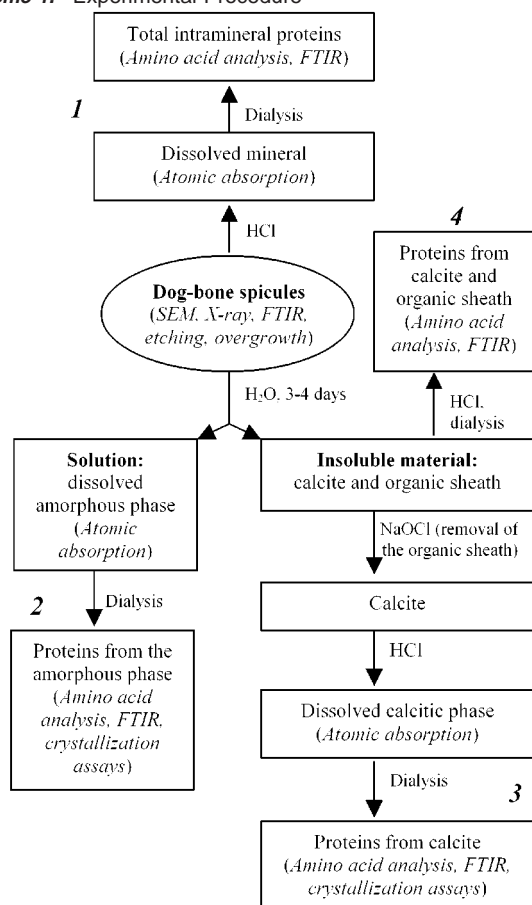
**Figure 2.** Tunic (dogbone) spicules formed by *P. pachydermatina*. Parts (a)–(d) reflect different stages of spicule development. Spicules are obtained by differential density centrifugation. The density of the fractions decreases from (a) to (d). Inset in (a,b): High magnification of the surface morphology, revealing steps of the calcitic {011} faces.

(Figure 2), small pieces of stalk tunic were placed in a vial containing 5.25% sodium hypochlorite solution and shaken at 60 oscillations/min with an electric shaker for 2 days. The specimens were then rinsed several times with double-distilled water (DDW) and air-dried. Dry spicules stored in glass containers were sent for characterization.

**Characterization of Spicules (Scheme 1). (i) Electron Microscopy.** The skeletal elements were examined in a JEOL 6400 scanning electron microscope (SEM) to verify surface cleanliness and structure.

- (12) Taylor, M. G.; Simkiss, K.; Greaves, G. N.; Okazaki, M.; Mann, S. *Proc. R. Soc. London* **1993**, B252, 75–80.
- (13) Vinogradov, A. P. *Chemical Composition of Marine Organisms*, Sears Foundation for Marine Research; Yale University: New Haven, CT, 1953.
- (14) Lambert, G.; Lambert, C. C.; Lowenstam, H. A. In *Skeletal Biomineralization: Patterns, Processes and Evolutionary Trends*; Carter, J. G., Ed.; Van Nostrand Reinhold: New York, 1990; Vol. 1, pp 461–469.
- (15) Aizenberg, J.; Lambert, G.; Addadi, L.; Weiner, S. *Adv. Mater.* **1996**, 8, 222–226.
- (16) Beniash, E.; Aizenberg, J.; Addadi, L.; Weiner, S. *Proc. R. Soc. London Ser. B—Biol. Sci.* **1997**, 264, 461–465.
- (17) Beniash, E.; Addadi, L.; Weiner, S. *J. Struct. Biol.* **1999**, 125, 50–62.
- (18) Addadi, L.; Berman, A.; Weiner, S. In *Mechanisms and Phylogeny of Mineralization in Biological Systems*; Suga, S., Nakahara, H., Eds.; Springer-Verlag: Tokyo, 1991; pp 29–33.
- (19) Albeck, S.; Aizenberg, J.; Addadi, L.; Weiner, S. *J. Am. Chem. Soc.* **1993**, 115, 11691–11697.
- (20) Aizenberg, J.; Hanson, J.; Ilan, M.; Leiserowitz, L.; Koetzle, T. F.; Addadi, L.; Weiner, S. *FASEB J.* **1995**, 9, 262–268.
- (21) Berman, A.; Addadi, L.; Weiner, S. *Nature* **1988**, 331, 546–548.
- (22) Berman, A.; Hanson, J.; Leiserowitz, L.; Koetzle, T. F.; Weiner, S.; Addadi, L. *Science* **1993**, 259, 776–779.
- (23) Aizenberg, J.; Hanson, J.; Koetzle, T. F.; Weiner, S.; Addadi, L. *J. Am. Chem. Soc.* **1997**, 119, 881–886.
- (24) Raz, S.; Weiner, S.; Addadi, L. *Adv. Mater.* **2000**, 12, 38–42.

## Scheme 1. Experimental Procedure



(ii) **X-ray Diffraction.** The diffraction spectrum was collected from a powdered sample using a Rigaku diffractometer with Cu K $\alpha$  radiation.

(iii) **Overgrowth Experiments.** The spicules were placed in a saturated solution of CaCO<sub>3</sub>, and calcite crystals were grown on the surfaces of spicules. The crystallographic orientation of the biogenic substrate was deduced from the morphology and the relative orientations of the epitaxially grown calcite rhombohedra.<sup>25</sup>

(iv) **Differential Density Sedimentation.** Tunic spicules were suspended in bromobenzene (density 1.497 g/mL) and were allowed to precipitate for 10 min. After sedimentation, the bromobenzene with the suspended lightest spicule fraction was removed, and spicules were washed, dried, and characterized. The precipitate was resuspended in a 1:1 mixture of bromobenzene and 1,2-dibromobenzene (density 1.956 g/mL), and the second spicule fraction was isolated as described for the first. Two heavy fractions were obtained by the resuspension of the second precipitate in 1,2-dibromobenzene, followed by the isolation of the suspension and the precipitate, respectively.

(v) **Infrared Spectroscopy.** Samples of ground spicules were dispersed in KBr pellets. Infrared absorption spectra were obtained using a MIDAC Fourier transform infrared (FTIR) spectrometer. The data presented are after subtraction of the corresponding KBr spectra.

(vi) **Etching Experiments.** The clean spicules were gently cut with a razor blade and immersed in DDW, 1 M KOH, or 2.5% NaOCl for 10 h with gentle rocking. After the treatment the spicules were briefly washed with DDW and dried, and the etch figures on the cross sections were observed in the SEM.

(vii) **Atomic Absorption Measurements.** The samples were measured using a Perkin-Elmer 5100 GFAAS atomic absorption spectro-

photometer. Control solutions with Ca<sup>2+</sup> concentrations of 5–50 ppm and Mg<sup>2+</sup> concentrations of 0.5–10 ppm were prepared from stock standard solutions of 500 and 1015 ppm (Aldrich), respectively. A powdered sample was dissolved in HNO<sub>3</sub> and diluted to fit into the calibration interval. Calcium and magnesium were determined independently after obtaining a linear calibration curve.

(viii) **Extraction of Intraskelatal Macromolecules.**<sup>19</sup> Clean, dry spicules were suspended in DDW, and concentrated hydrochloric acid was added dropwise over several hours to dissolve the mineral part. The final pH of the solution was 6.7. This solution was extensively dialyzed against DDW (Spectrapor 3 dialysis tubing) and lyophilized, to yield the total macromolecular fraction. An aliquot of the extract was hydrolyzed in 6 N HCl at 112 °C for 24 h, and the amino acid composition and protein concentration were determined by amino acid analysis (HP Aminoquant system).

(ix) **Independent Characterization of Amorphous and Calcitic Layers.** Independent characterization in dogbone spicules was performed after differential dissolution of the two phases as described in Scheme 1 (see Results for details).

**Crystallization Assays.** Calcium carbonate was precipitated in a Nunc multidish (4 × 6 wells with a diameter of 1.5 cm). A total volume of 1.5 mL of 25 mM calcium chloride solution was introduced into each well. Aliquots of concentrated protein solutions were added to the above CaCl<sub>2</sub> solution. The effect of Mg<sup>2+</sup> was studied by adding various amounts of MgCl<sub>2</sub>. The multidish was placed into closed desiccator containing vials of ammonium carbonate for 24 h. In each experiment, controls that contained the pure calcium chloride solution without additives were analyzed.<sup>19,25</sup> The precipitates were lightly rinsed with DDW, dried, and characterized by SEM, FTIR, and electron diffraction in a transmission electron microscope (TEM).

To estimate the yield and Mg content of synthetic ACC grown in the presence of macromolecules, the amounts of Ca<sup>2+</sup> and Mg<sup>2+</sup> were measured by atomic absorption in the mother liquor, in the solution that underwent precipitation, and in the dissolved precipitate. Precipitation from a 1:1 mixture of a 25 mM solution of CaCl<sub>2</sub> and a 25 mM solution of MgCl<sub>2</sub> was studied. The protein content and composition of synthetic ACC were determined from amino acid analysis of the dissolved precipitate.

## Results

**Spicules from the Ascidian *P. pachydermatina*.** The antler-shaped body spicules (Figure 1) are composed entirely of stabilized amorphous calcium carbonate.<sup>15</sup> In water, the spicules' smooth surfaces are preserved intact. Etching with KOH reveals shapeless etch pits on the surfaces and a regular pattern of concentric rings on the cross sections. The amorphous character of these spicules was inferred from high-resolution powder X-ray diffraction that showed no discernible peaks and was confirmed by FTIR that showed broad  $\nu_2$  and  $\nu_1$  absorption bands of ACC at 866 and 1070 cm<sup>-1</sup>, respectively, and the split of the  $\nu_3$  band around 1450 cm<sup>-1</sup> (Figure 3a).<sup>26</sup>

The tunic spicules produced by the same organism (Figure 2) were reported to be composed of a single calcite crystal.<sup>14</sup> The mature spicules have a typical dogbone shape with rough surfaces that exhibit {011} calcitic steps (Figure 2a). X-ray powder diffraction of the intact spicules showed only the characteristic calcitic reflections. The FTIR spectrum also showed only the characteristic, although slightly broadened  $\nu_4$ ,  $\nu_2$ , and  $\nu_3$  absorption bands of calcite<sup>26</sup> at 714, 876, and around 1435 cm<sup>-1</sup>, respectively (Figure 3c). The single crystalline nature of the dogbone spicules was demonstrated using polarized light microscopy studies: the spicules are birefringent and extin-

(25) (a) Okazaki, K.; Dillaman, R. M.; Wilbur, K. M. *Biol. Bull.* **1981**, *161*, 402–415. (b) Aizenberg, J.; Albeck, S.; Weiner, S.; Addadi, L. *J. Cryst. Growth* **1994**, *142*, 156–164.

(26) Chester, R.; Elderfield, H. *Sedimentology* **1967**, *9*, 5–21.

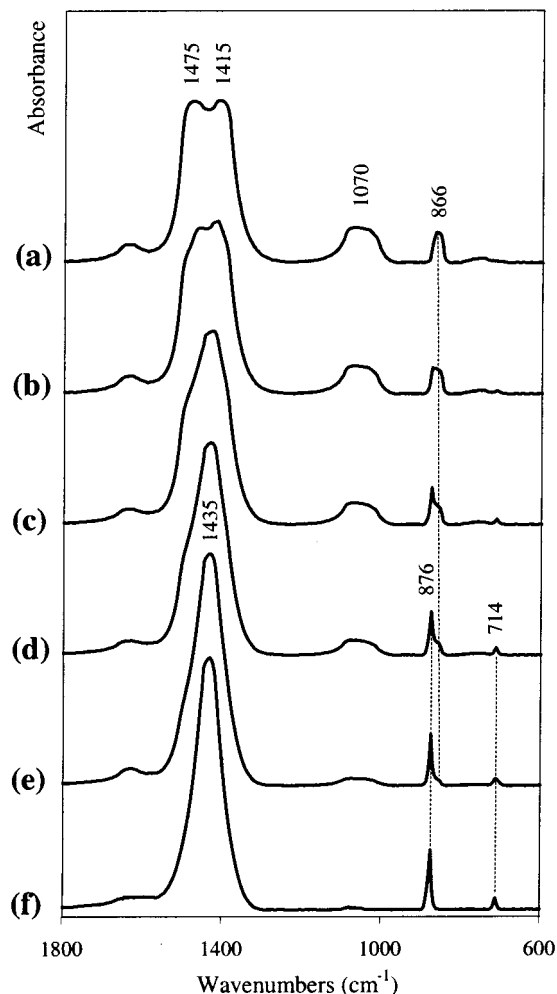


**Figure 3.** Infrared spectra of skeletal elements from *P. pachydermatina*. (a) Body (antler) spicules are composed entirely of stabilized amorphous CaCO<sub>3</sub>. (b–e) Tunic (dogbone) spicules at different stages of development: (b) spicules in the lightest fraction of the differential density centrifugation experiment (see Figure 2d) are mostly composed of ACC; (c) the calcitic component is apparent in the fraction shown in Figure 2c; (d) the calcitic component further increases in the fraction shown in Figure 2b; (e) mature spicules (see Figure 2a) are mostly calcitic. (f) Reference spectrum of pure calcite.

gush uniformly. Single-crystal X-ray analysis of individual spicules did not, however, reveal diffraction peaks of the intensity expected from a calcite single crystal of equivalent volume.

To further characterize the crystallographic nature of the spicules, we carried out overgrowth experiments,<sup>25</sup> in which synthetic calcite crystals were grown epitaxially on the spicule surfaces (Figure 4). The *c* crystallographic axes of the newly formed calcite rhombohedra all coincide with the spicule axis, providing the explanation for the observed birefringence. The crystals are, however, slightly misaligned in the *a,b*-plane (Figure 4).

In the overgrowth experiments, we noticed that calcite crystals do not overgrow the broken cross sections of the spicules. This observation raised the possibility that the inner part of the spicule is composed of a mineral other than calcite and is presumably amorphous, as no other crystalline phases were detected in the diffraction pattern. The surfaces of dry, freshly sectioned spicules are smooth and show no indication of structural boundaries (Figure 5a). After exposure to DDW for 3–5 h, the inner part of the spicule starts to corrode (Figure 5b), revealing

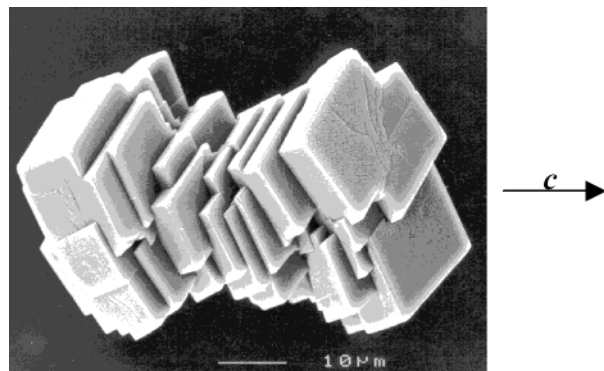


**Figure 4.** Dogbone spicule epitaxially overgrown by synthetic calcite crystals. Note that the edges of the crystals are not perfectly parallel to each other, indicating that their biogenic substrate is a polycrystalline aggregate with a preferred *c*-axis orientation and misalignment in the *a,b*-plane.

an insoluble organic sheath stretched between the outer calcitic layer and the inner amorphous core (Figure 5c). The dispositions of the outer and inner layers are even more apparent after KOH etching (Figure 5d). Upon heating (>100 °C), the core loses water and recrystallizes into calcite, as was confirmed by spectroscopic data. The recrystallized calcite is oriented epitaxially with the calcitic envelope (Figure 5e). Bleaching the original spicules that did not undergo recrystallization in a 2.5% NaOCl solution for 1 day completely dissolves the core and the surrounding organic sheath (Figure 5f). On the basis of the above observations, we deduce that the dogbone spicule is a composite tissue, in which a crystalline envelope encloses an amorphous core.

Differential density centrifugation of the tunic extract showed four distinctive spicule types (Figure 2). The mineral composition of the different spicule types was characterized using FTIR (Figure 3). The cylindrical structures in the lightest fraction (Figure 2d) appear to be composed mostly of amorphous calcium carbonate (Figure 3b). Those in the denser fractions (Figure 2b,c) are more crystalline (Figure 3c,d). We therefore believe that these density fractions represent different stages of spicule formation, with the smallest, least dense amorphous ones being the first formed precipitate. The mature dogbone spicules (Figure 2a) are mostly calcitic (Figure 3e).

**Differential Analysis of Amorphous and Calcitic Layers in Dogbone Spicules.** The intact spicules (1), ACC core (2), calcitic envelope (3), and the organic sheath separating the two phases (4) were differentially dissolved and characterized independently by atomic absorption and amino acid analyses (see Scheme 1). A weighed amount (50 mg) of dried, crushed dogbone spicules was suspended in DDW for 3–4 days and placed on a rocking table in a cold room (4–5 °C). This treatment resulted in a differential, quantitative dissolution of amorphous calcium carbonate. The insoluble spicule material was air-dried and weighed (42.6 mg) to estimate the fraction of ACC inside the composite spicule tissue. An aliquot of the solution was analyzed by atomic absorption to yield the Mg content in the amorphous phase. Extensive dialysis of the solution followed by lyophilization yielded the fraction of macromolecules that is associated with the amorphous calcium carbonate phase and, possibly, soluble proteins from the separating organic sheath. After dissolution of the amorphous core and removal of the corresponding macromolecules, one-

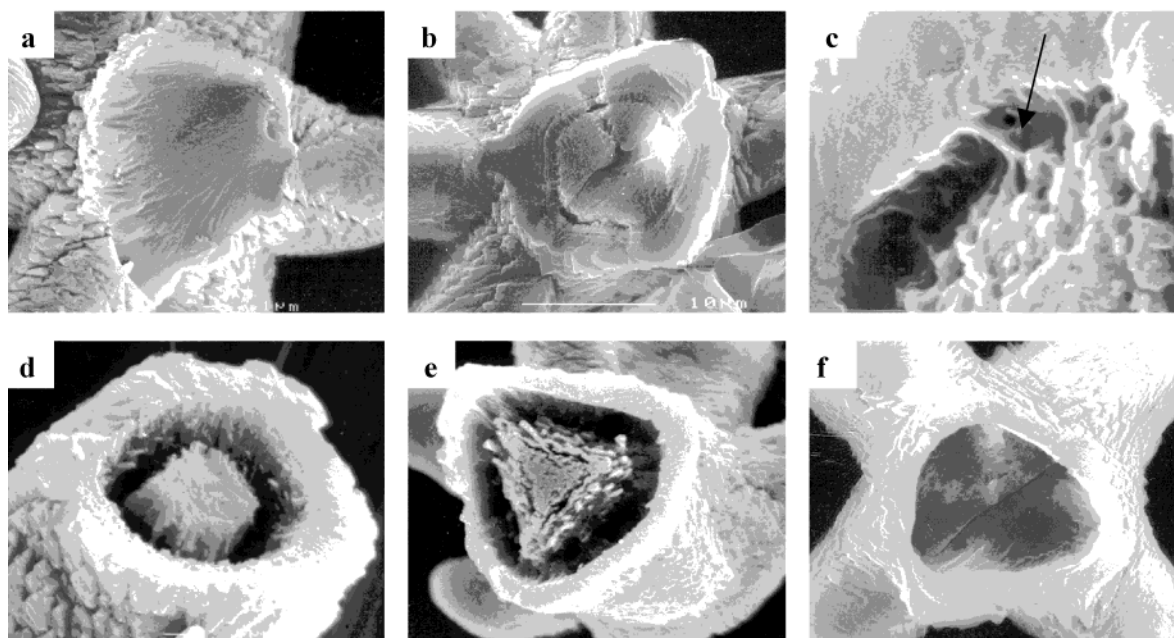


**Figure 5.** Chemical treatments of dogbone spicules reveal the combination of two mineral phases—the ACC core and the calcitic envelope separated by an organic sheath. (a) Freshly cut, untreated spicule with a homogeneous cross section. (b) Slight etching of the inner core in DDW. (c) High magnification of the phase boundary showing an insoluble organic layer (arrow). (d) Selective dissolution of the core material in KOH. (e) Recrystallization of the ACC core into oriented calcite upon heating (note the 3-fold symmetry of the recrystallized calcitic structure). (f) Complete removal of the ACC and organic layer in a 2.5% NaOCl solution. Only the calcitic phase remains.

**Table 1.** Protein Concentrations, Amino Acid Compositions, and Mg Contents in Various Biogenic Amorphous and Crystalline  $\text{CaCO}_3$  Phases

	dogbone spicules				antler spicules, intact <sup>15</sup>	sponge spicules, ACC part <sup>15</sup>	sponge spicules, calcitic part <sup>15</sup>
	intact spicule (1) <sup>a</sup>	ACC core (2) <sup>a</sup>	calcitic layer (3) <sup>a</sup>	organic sheath and calcite (4) <sup>a</sup>			
mineral, mg	50.0	7.4	21.3	21.3	10.0	12.1	2.9
protein, $\mu\text{g}^b$	22.8	3.6	1.9	9.3	9.1	16.3	1.8
protein concn, wt % of mineral	0.046	0.049	0.009	0.044	0.091	0.135	0.062
Mg content, mol % <sup>c</sup>	2.55	5.9	1.7		9.1	11.2	6.4
amino acid, mol % of protein							
Asx	10.9	7.1	18.8	11.7	7.8	7.2	28.5
Glx	12.1	17.2	8.0	11.4	16.8	17.7	14.3
Ser	7.7	11.2	6.8	7.3	18.0	19.2	8.8
Thr	13.2	12.2	4.6	13.2	4.6	4.3	3.5
Gly	11.0	12.6	20.8	11.2	19.6	19.9	10.8
Ala	6.8	5.5	6.5	7.3	8.0	8.4	10.5
Val	5.9	6.0	4.6	6.2	3.5	3.5	3.5
Leu	5.3	5.3	7.1	5.6	3.5	2.3	2.9
Ile	3.3	3.0	1.2	3.7	2.4	1.7	2.0
Arg	5.0	8.9	3.4	3.7	2.3	1.1	2.0
Lys	7.2	4.4	4.0	7.9	3.0	4.1	1.7
His	1.5		0.8	1.8	3.1	3.2	1.1
Phe	3.4	3.3	1.2	3.7	1.7	1.0	2.3
Tyr	0.9	0.4	2.2	0.6	1.8	0.8	1.6
Cys	1.7	1.6	7.8	1.8	0.1		0.2
Met	0.9		1.2	0.9	0.6		2.1
Pro	3.1	1.2	1.0	2.1	3.2	5.4	4.2

<sup>a</sup> Origins of fractions 1–4 are shown in Scheme 1. <sup>b</sup> Based on amino acid analysis. <sup>c</sup> Based on atomic absorption measurements.

half of the remaining insoluble spicule material (21.3 mg) was treated with 2.5% sodium hypochlorite solution to dissolve the insoluble organic sheath between amorphous and crystalline layers. The residual calcitic material was dissolved in HCl. An aliquot of the solution was analyzed by atomic absorption to obtain the Mg content in the crystalline phase. The solution was then dialyzed and lyophilized, to yield macromolecules associated with the calcitic phase. The other half (21.3 mg) of the remaining insoluble spicule material was dissolved in HCl to solubilize calcite. The insoluble material obtained—the

organic sheath that separates the amorphous and crystalline phases and insoluble proteins from the calcitic layer (insignificant fraction)—was removed by centrifugation. This experiment was repeated several times, and the results are representative. The results are summarized in Table 1.

The fraction of amorphous calcium carbonate in the composite tissue of the dogbone spicules ( $\%_{\text{ACC}}$ ) was estimated using two approaches. (i) From the weight loss in the differential dissolution experiment (Table 1):  $\%_{\text{ACC}} \approx 15\%$ . Because of the possibility of incomplete dissolution of ACC, this value presents

the lower estimate of the ACC fraction. (ii) From atomic absorption measurements of the Mg content in the intact spicules relative to the known Mg content of the amorphous and calcitic layers (Table 1): %<sub>ACC</sub> ≈ 20%.

The Mg contents are 5.9 and 1.7 mol % in the ACC core and the calcitic layer, respectively. The concentrations of intramineral proteins in the two mineral phases are 0.05 and 0.01 wt %, respectively (Table 1). The amino acid composition of macromolecules associated with the ACC part of the dogbone spicules revealed proteins rich in glutamic acid and hydroxyamino acids (threonine and serine). The macromolecular extract from the calcitic envelope was characteristically rich in aspartic acid (Table 1).

The amino acid analyses of the macromolecular extracts from the ACC phases also revealed an elution peak characteristic of a certain non-amino-acid residue (~10 mol % of total amino acids), which was absent in the elution profiles of the macromolecules from the calcitic phases. We suspect that this peak originates from the polysaccharide moieties. This is supported by the FTIR spectra of different macromolecular fractions that showed pronounced broad absorption peaks in the polysaccharide region (around 1100 cm<sup>-1</sup>) for the macromolecules from all biogenic ACC phases and an insignificant peak in this area for the macromolecules from biogenic calcite (Figure 6). The two absorption peaks at 1213 and 1155 cm<sup>-1</sup> in the spectra obtained from the organic sheath (Figure 6b) are reminiscent of sulfate. This suggests that some of the macromolecules are sulfated. Furthermore, the spectrum of the macromolecules from the ACC part of the spicules (Figure 6c) contains peaks, such as 658 and 602 cm<sup>-1</sup>, which are characteristic of gypsum (CaSO<sub>4</sub>·2H<sub>2</sub>O). This indicates that sulfate as well as calcium was present in the original solution and upon drying must have precipitated out.

**In Vitro Precipitation of CaCO<sub>3</sub> Controlled by Specialized Macromolecules.** To study the possible role of intraskeletal macromolecules in the stabilization of ACC and in the formation of the composite ACC/calcite tissues, the macromolecules associated with the two mineral phases were assayed for their effect on the precipitation of CaCO<sub>3</sub> in vitro. The addition of macromolecules extracted from the calcitic layer of dogbone spicules to solutions saturated with respect to CaCO<sub>3</sub> reduced the induction time for the crystallization process relative to the control experiments carried out without any additives from ~1 h to ~20 min. The crystals formed are calcite with modified morphology. In addition to the normal {104} cleavage planes of pure calcite, these crystals exhibited well-developed stepped faces slightly oblique to the *c* crystallographic axis, indexed as {01*l*} (*l* ≈ 1.5) (Figure 7a). This modified crystal morphology correlates well with the expression of the similar family of calcite faces on the surfaces of the dogbone spicules (Figure 2a,b).

Macromolecules extracted from the amorphous core of the dogbone spicules caused the complete inhibition of crystallization for at least 1–2 weeks at protein concentrations of 1–4 μg/mL, both in the presence and in the absence of Mg. At protein concentrations of <1 μg/mL, sporadic calcite crystals were observed.

The formation of spherical particles of stabilized synthetic ACC was observed with the addition of macromolecules extracted from the stable amorphous calcium carbonate of the

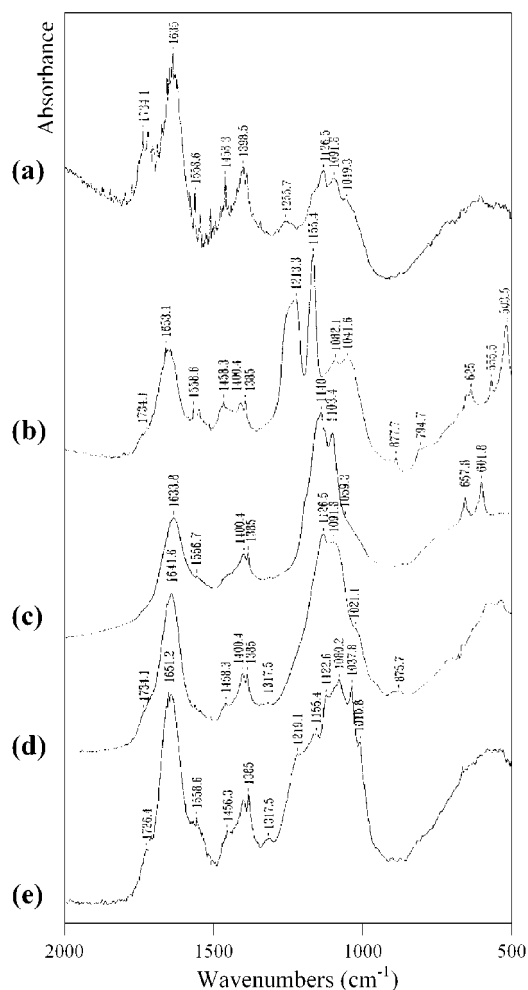


**Figure 6.** Infrared spectra of specialized macromolecules differentially extracted from different biogenic CaCO<sub>3</sub> phases. (a) Macromolecules from the calcitic layer of dogbone spicules. (b) Insoluble organic sheath in dogbone spicules. (c) Macromolecules from the ACC core of dogbone spicules. (d) Macromolecules from the ACC of antler spicules. (e) Macromolecules from the ACC layer of the composite ACC/calcitic spicules formed by the calcareous sponge *Clathrina*. Note the broad sugar bands around 1100 cm<sup>-1</sup> in (c)–(e), suggesting that the proteins associated with various biogenic ACC phases are all heavily glycosylated, while those extracted from the calcite layer are less glycosylated.

antler spicules<sup>15</sup> (Figure 7b). The electron diffraction pattern of the precipitate embedded in vitrified ice<sup>17</sup> showed only diffuse amorphous bands. The formation of ACC in the precipitate was confirmed by FTIR.

The yield (*Y*, %) of synthetic ACC formed in the presence of macromolecules extracted from antler spicules with or without Mg ions was estimated by atomic absorption (i) from the difference in the Ca contents between the solutions before and after precipitation and (ii) directly from the yield of dissolved precipitate: *Y* ≈ 15–20%. The Mg content (*X*, mol %) in the synthetic amorphous precipitate was ≈8.5 mol %. In the absence of Mg, the precipitation of stabilized ACC occurred at protein concentrations of >1 μg/mL in the crystallization solution. Lower protein concentrations were required when Mg was present in the mother liquor (Ca/Mg = 1): the precipitation of stabilized ACC occurred at protein concentrations of >0.5 μg/mL. To determine the protein fraction in the synthetic ACC, the precipitate was quantitatively dissolved and dialyzed, and the released macromolecules were characterized by amino acid

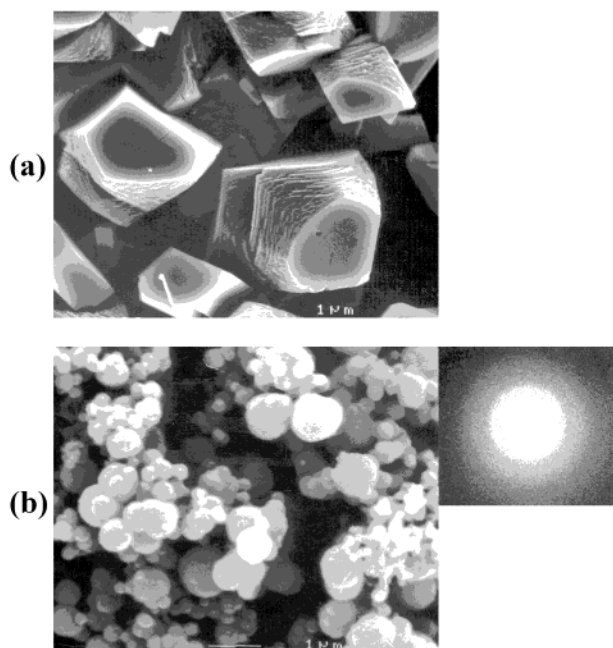


**Figure 7.** SEM of synthetic  $\text{CaCO}_3$  grown in the presence of the specialized macromolecules. (a) Calcite crystals grown with the addition of proteins from the calcitic layer of dogbone spicules. (b) Synthetic ACC stabilized by the proteins extracted from antler spicules. Inset: Electron diffraction pattern showing its amorphous character.

analysis. The estimated protein content was 0.12 wt % when the precipitation was carried out in the absence of Mg and 0.07 wt % in the presence of Mg.

We also studied the templating properties of the insoluble organic sheath that we found between the amorphous and calcitic phases in the dogbone spicules (Figure 5c). The purified macromolecular fraction was adsorbed on a glass cover slip,<sup>27</sup> which was then introduced into a solution saturated with respect to  $\text{CaCO}_3$ . The cover slip overgrown with calcite crystals was directly mounted in a diffractometer and analyzed in the  $\theta$ - $2\theta$  scan mode. In this mode, only diffracting planes parallel to the plane of the substrate (nucleating planes) produce significant diffraction intensity. The peaks in the XRD profile represent, therefore, the predominant crystallographic orientations of the crystals. X-ray analysis of calcite crystals grown on the insoluble organic sheath showed a pronounced increase in the relative intensity of the  $\{110\}$ ,  $\{300\}$ ,  $\{012\}$ , and  $\{202\}$  diffraction peaks and a decrease in the intensity of the  $\{104\}$ ,  $\{018\}$ ,  $\{116\}$ , and  $\{113\}$  peaks (Figure 8). This implies that the insoluble organic sheath induces the preferential nucleation of calcite crystals from the crystallographic planes roughly parallel to the  $c$ -axis.

## Discussion

Our attention was drawn to the ascidian *P. pachydermatina* because it produces skeletal elements from two different materials: body spicules composed entirely of amorphous calcium carbonate (Figure 1) and tunic spicules composed of crystalline calcite (Figure 2).<sup>14</sup> This organism therefore presents an attractive candidate for the comparison of macromolecules and ions involved in the formation of ACC and calcite in the same organism.

Our study showed that the tunic spicules, which were reported to be single calcite crystals,<sup>14</sup> are, in fact, complex composite

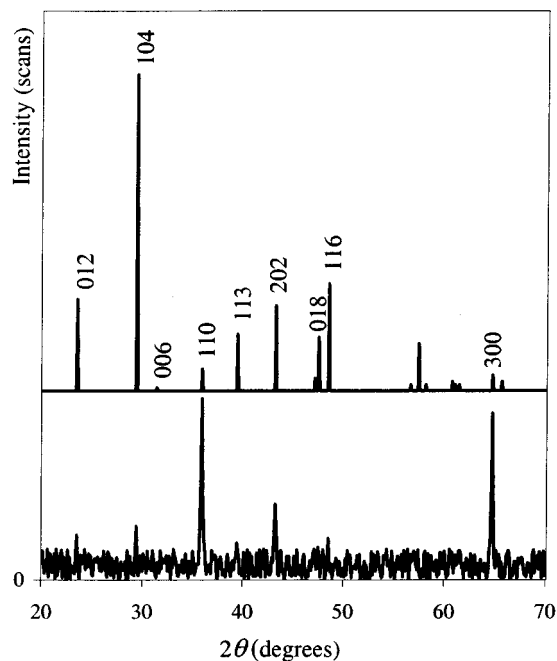


**Figure 8.** Powder X-ray diffraction analysis of synthetic calcite crystals grown on the adsorbed layer of insoluble macromolecules that separate the amorphous and crystalline phases in the dogbone spicules (bottom) and the reference diffraction pattern of randomly oriented calcite powder (top). Note the predominant  $\{hk0\}$  reflections in the synthetic crystals grown on the organic layer.

tissues, with well-defined domains of amorphous and crystalline calcium carbonates separated by an organic layer. The crystalline envelope forms around the ACC core and comprises 80–85 wt % of the mature spicules. It is composed of polycrystalline calcite with preferred  $c$ -axes orientations roughly parallel to the morphological axis of the spicule.

The Mg content in the ACC core is significantly higher than that in the calcitic layer in dogbone spicules, implying that Mg ion is an important factor regulating the formation of different calcium carbonate phases. It is possible that sulfate ions are present in the ACC phase and are covalently bound to parts of the organic matrix. It is interesting to note that a water-soluble chitin sulfate-rich polysaccharide has been identified in the test of a tunicate,<sup>28</sup> suggesting that sulfate ions may also play a role in the mineralization process.

The protein content in the ACC core is higher than that in the calcitic layer. The amino acid compositions of macromolecules associated with the two mineral phases are quite different. The macromolecules occluded in the crystalline layer are rich in aspartic acid, as is typical of many other calcitic and aragonitic mineralized tissues.<sup>1,29,30</sup> The macromolecular extract from the ACC core is rich in glutamic and hydroxyamino acids (threonine and/or serine) and, possibly, sugar. This is similar to the macromolecules extracted from antler spicules and the sponge spicules of *Clathrina* (Table 1).<sup>15</sup> The sponges and the ascidians are widely separated in the animal kingdom phylogenetic tree,

(27) Addadi, L.; Weiner, S. *Proc. Natl. Acad. Sci. U.S.A.* **1985**, *82*, 4110–4114.

(28) Anno, K.; Otsuko, K.; Seno, N. *Biochim. Biophys. Acta* **1974**, *362*, 215–219.

(29) Mann, S. In *Biomaterialization. Chemical and Biochemical Perspectives*; Mann, S., Webb, J., Williams, R. J. P., Eds.; VCH Publishers: Weinheim, 1989; pp 189–222.

(30) (a) Addadi, L.; Weiner, S. *Angew. Chem.* **1992**, *31*, 153–169. (b) Albeck, S.; Weiner, S.; Addadi, L. *Chem Eur. J.* **1996**, *2*, 278–284.

and yet they are strikingly similar in this very basic aspect of their mineralization processes. Our results suggest that the choice of the acidic functionality (aspartic or glutamic acid) plays an essential role in the regulation of the formation of calcite or ACC. It would be interesting to further verify whether the ACC proteins enriched in hydroxyamino acids may, in fact, have phosphorylated serine and threonine residues, an important modulatory functionality.<sup>6</sup>

Our results on *in vitro* precipitation of CaCO<sub>3</sub> show that the macromolecules from all three biogenic ACC phases—ACC core in dogbone spicules, antler spicules, and ACC envelope in sponge spicules—inhibit the formation of calcite, which would normally crystallize out of a saturated CaCO<sub>3</sub> solution. This implies that the macromolecules from these phases contain calcite crystallization inhibitors. Moreover, macromolecules extracted from the antler spicules and the ACC layer of the sponge spicules induced the formation of stable ACC in the precipitation assays. In contrast, the macromolecules extracted from the ACC core of the dogbone spicules did not induce a precipitate. It is, however, possible that a less stable form of ACC precipitated transiently and then dissolved. Thus, the dogbone ACC apparently does not contain macromolecules capable of fully stabilizing ACC *in vitro*. We do note that the mature antler and sponge ACC phases are stable in aqueous solutions, whereas the dogbone ACC readily dissolves. There is thus a correlation between the biologically formed materials and the corresponding *in vitro* products.

*In vitro* crystallization in the presence of macromolecules extracted from the calcitic layer of the dogbone spicules resulted in the formation of calcite crystals with a modified morphology similar to that expressed in the original spicules, including the development of crystal faces that are not normally expressed in synthetic calcite crystals. This implies that intracrystalline macromolecules are involved in the formation and shaping of the calcitic phase.<sup>19</sup> It should be emphasized that the *in vitro* experiments are clearly different from the more complex processes of mineral formation *in vivo*. Nevertheless, our experiments clearly show that specific macromolecular ensembles,

each with its distinct effect, are involved in the formation of the amorphous and crystalline CaCO<sub>3</sub>.

On the basis of our observations, we suggest a scenario for the development of the complex composite ACC/calcite tissue of dogbone spicules. It has been shown that spicules form extracellularly within a closed compartment surrounded by an epithelium of sclerocytes.<sup>14</sup> We believe that the formation starts with the deposition of amorphous calcium carbonate induced by specialized macromolecules, rich in sugar, glutamic acid, and hydroxyamino acids that are secreted into the compartment. The amorphous phase is further stabilized and protected by the insoluble organic cover. We have indeed observed such amorphous structures in the lightest fraction produced by differential density centrifugation of the tunic extract (Figure 2d). The organic envelope then templates a layer of calcitic plates with preferred *c*-axis orientation (Figure 2c). A different macromolecular ensemble, rich in aspartic acid, modulates the morphology of the calcitic layer. This results in the development of a specific surface structure and texture of the spicules (Figure 2a,b).

We can only speculate on how the organism may benefit from the presence of skeletal elements, in which amorphous and crystalline phases coexist. Amorphous materials are isotropic and generally less brittle, while their crystalline counterparts are harder and less soluble. It is, therefore, conceivable that composite amorphous/crystalline structures possess advantageous mechanical properties, which may be interesting to investigate. This information, together with an understanding of the mechanisms by which ACC is stabilized and the manner in which the spicules form, may provide new strategies for fabricating novel synthetic materials with improved properties.

**Acknowledgment.** L.A. is the incumbent of the Dorothy and Patrick Gorman Professorial Chair in Biological Ultrastructure. S.W. has the Dr. Walter and Dr. Trude Borchardt Professorial Chair in Structural Biology.

JA016990L